New Test Beam Results of 3D and Pad Detectors Constructed with Poly-Crystalline CVD Diamond

M. Reichmann[z,*], A. Alexopoulos[c], M. Artuso[t], F. Bachmair[x], L. Bäni[x], M. Bartosik[c], J. Beacham[m], H. Beck[w], V. Bellini[b], V. Belyaev[l], B. Bentele[s], P. Bergonzo[k], A. Bes[aa], J-M. Brom[g], M. Bruzzi[d], G. Chiodini[z], D. Chren[r], V. Cindro[i], G. Claus[g], J. Collot[aa], J. Cumalat[s], A. Dabrowski[c], R. D'Alessandro[d], D. Dauvergne[aa], W. de Boer[j], S. Dick[m], C. Dorfer[x], M. Dünser[c], G. Eigen[ad], V. Eremin[f], J. Forneris[o], L. Gallin-Martel[aa], M.L. Gallin-Martel[aa], K.K. Gan[m], M. Gastal[c], C. Giroletti[q], M. Goffe[g], J. Goldstein[q], A. Golubev[h], A. Gorišek[i], E. Grigoriev[h], J. Grosse-Knetter[w], A. Grummer[u], M. Guthoff[c], B. Hiti[i], D. Hits[x], M. Hoeferkamp[u], T. Hofmann[c], J. Hosslet[g], J-Y. Hostachy[aa], F. Hügging[a], C. Hutton[q], J. Janssen[a], H. Kagan[m], K. Kanxheri[ab], R. Kass[m], M. Kis[e], G. Kramberger[i], S. Kuleshov[h], A. Lacoste[aa], S. Lagomarsino[d], A. Lo Giudice[o], E. Lukosi[y], C. Maazouzi[g], I. Mandic[i], A. Marino[s], C. Mathieu[g], M. Menichelli[ab], M. Mikuž[i], A. Morozzi[ab], J. Moss[ac], R. Mountain[t], S. Murphy[v], M. Muškinja[i], A. Oh[v], P. Oliviero[o], D. Passeri[ab], H. Pernegger[c], R. Perrino[z], F. Picollo[o], M. Pomorski[k], R. Potenza[b], A. Quadt[w], F. Rarbi[aa], A. Re[o], G. Riley[ab], S. Roe[c], D.A. Sanz-Becerra[x], M. Scaringella[d], D. Schaefer[c], C.J. Schmidt[e], E. Schioppa[c], S. Schnetzer[n], S. Sciortino[d], A. Scorzoni[ab], S. Seidel[u], L. Servoli[ab], D.S. Smith[m], B. Sopko[r], V. Sopko[r], S. Spagnolo[z], S. Spanier[y], K. Stenson[s], R. Stone[n], B. Stugo[ad], C. Sutera[b], M. Traeger[e], D. Tromson[k], W. Trischuk[p], C. Tuve[b], J. Velthuis[q], N. Venturi[c], E. Vittone[o], S. Wagner[s], R. Wallny[x], J.C. Wang[t], C. Weiss[c], N. Wermes[a], M. Yamouni[aa], M. Zalieckas[ad], M. Zavrtanik[i]

[a]Universität Bonn, Bonn, Germany, [b]INFN/University of Catania, Catania, Italy, [c]CERN, Geneva, Switzerland, [d]INFN/University of Florence, Florence, Italy, [e]GSI, Darmstadt, Germany, [f]Ioffe Institute, St. Petersburg, Russia, [g]IPHC, Strasbourg, France, [h]ITEP, Moscow, Russia, [i]Jožef Stefan Institute, Ljubljana, Slovenia, [j]Universität Karlsruhe, Karlsruhe, Germany, [k]CEA-LIST Technologies Avancees, Saclay, France, [l]MEPHI Institute, Moscow, Russia, [m]The Ohio State University, Columbus, OH, USA, [n]Rutgers University, Piscataway, NJ, USA, [o]University of Torino, Torino, Italy, [p]University of Toronto, Toronto, ON, Canada, [q]University of Bristol, Bristol, UK, [r]Czech Technical University, Prague, Czech Republic, [s]University of Colorado, Boulder, CO, USA, [t]Syracuse University, Syracuse, NY, USA, [u]University of New Mexico, Albuquerque, NM, USA, [v]University of Manchester, Manchester, UK, [w]Universität Göttingen, Göttingen, Germany, [x]ETH Zürich, Zürich, Switzerland, [y]University of Tennessee, Knoxville, TN, USA, [z]INFN-Lecce, Lecce, Italy, [aa]LPSC-Grenoble, Grenoble, France, [ab]INFN-Perugia, Perugia, Italy, [ac]California State University, Sacramento, CA, USA, [ad]University of Bergen, Bergen, Norway,

---

Abstract

The RD42 collaboration is investigating Chemical Vapour Deposition (CVD) diamond as a future material for particle detectors in a harsh radiation environment. The latest beam test results of 3D pixel detectors fabricated with poly-crystalline CVD (pCVD) diamonds are discussed. The cells of the devices have a size of $50\,\mu m \times 50\,\mu m$ with columns $2.6\,\mu m$ in diameter. The cells were ganged in a 3×2 and a 5×1 pattern to match the layouts of the pixel read-out chips currently used in the CMS and ATLAS experiments at the LHC, respectively. In beam tests, using tracks reconstructed with a high precision tracking telescope, both devices achieved tracking efficiencies greater than 97 %. The efficiency of both devices plateaus at a bias voltages of 30 V. The latest high rate beam test results of irradiated pCVD diamond pad detectors are also presented. In many measurements with with particle fluxes up to $20\,\mathrm{MHz/cm^2}$ and irradiations up to $8 \cdot 10^{15}\,\mathrm{n/cm^2}$ it could be shown that irradiated pCVD diamonds do not depend on flux to the $\mathcal{O}(2\,\%)$.

Keywords: Diamond Detectors, 3D, Rate

---

1. Introduction

The radiation levels of the High-Luminosity LHC (HL-LHC) will become a big challenge for the future detectors. By 2028 an instantaneous luminosity of $5 \cdot 10^{34}\,\mathrm{cm^{-2}\,s^{-1}}$ is expected [1]. In this environment the innermost tracking layer at a distance of ~30 mm to the interaction point is expected to be exposed to a total fluence of $2 \cdot 10^{16}\,\mathrm{n_{eq}/cm^2}$ [2].

After large fluence, all detector materials become trap limited with a mean drift distance below $75\,\mu m$. Due to its properties, such as the displacement energy of 42 eV/atom and the band gap of 5.5 eV, the RD42 collaboration is investigating CVD diamond possible detector material [3]. In various studies it was shown that compared to corresponding silicon detectors, diamond is at a minimum three

*Corresponding author

times more radiation hard [4], collecting the charges at least two times faster [5] and conducting heat four times more efficiently [6].

By now the technology of diamond detectors is well established in high energy physics. Many high energy physics experiments are already using Beam Condition Monitors or Beam Loss Monitors based on CVD diamonds [7], [8], [9].

The RD42 collaboration is also investigating a novel detector design, namely 3D detectors. This concept is a possible way to reduce the drift distance below the mean drift distance of an irradiated sensor without reducing the total number of the excited electron-hole pairs. Since the particle flux of the HL-LHC will be in completely new regime, high rate studies of pad detectors are performed at Paul Scherrer Institut (PSI) with nearly minimum ionising particles (MIPs) and tunable particle fluxes up to $\mathcal{O}\left(10\,\mathrm{MHz/cm^2}\right)$.

2. 3D Pixel Detectors

The 3D geometry reduces the drift distance of the charge carriers created by ionising particles compared to a planar device. More details about the working principle can be found in [10], [11].

2.1. Fabrication

In order to generate the electrodes in diamond columns are drilled using a 130 fs laser with a wavelength of 800 nm which converts the diamond into a electrically conductive mixture of different carbon phases [12]. The conductivity of the columns is of the $\mathcal{O}\,(1\,\Omega\,\mathrm{cm})$. By applying Spacial Light Modulation (SLM) a column yield of >99 % and a column diameter of 2.6 µm can be achieved [13]. The largest fabricated device has about 4000 of these cells.

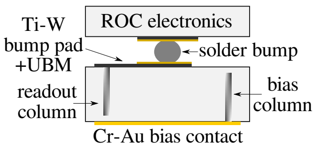

Figure 1: Bump bonding scheme.

The final device was built by connecting to the bias and readout columns with surface metallisation and bump bonding the sensor to the readout electronics as shown in Figure 1. For the detectors described in here a cell size of 50 µm × 50 µm was chosen. Since the layout of the available readout chips (ROCs) has a different pixel pitch several cells had to be ganged together.

2.2. PSI46digV2.1respin read-out

The first prototype of a 50 µm × 50 µm 3D pixel detector was connected to the PSI46digV2.1respin ROC [14] with a 3 × 2 cell ganging to match the pixel pitch of 150 µm × 100 µm. In this case the 3D sensors were bump bonded to the ROC at the Nanofabrication Lab in Princeton with indium bumps. The preliminary beam test results show, that relative to a planar silicon device the efficiency

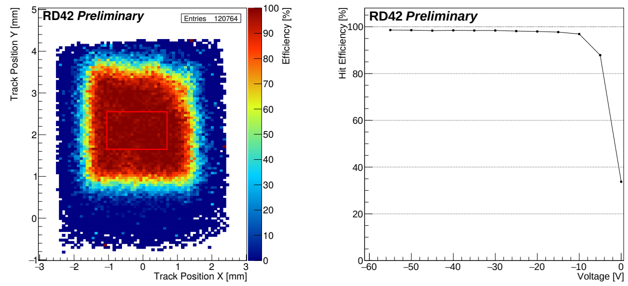

(a) 3 × 2 efficiency. (b) Efficiency vs. voltage.

Figure 2: 3 × 2 results.

in the red fiducial area amounts to 99.3 % (Figure 2a). It was not considered that some of the 3D cells in this region may not work due to broken or missing columns or due to metalisation issues. In order to acquire this information further data has to be analysed. Nevertheless a small mismatch is expected due to low field regions between the electrodes and the columns themselves. Figure 2b shows the device is already fully efficient at a Voltage of 30 V. The preliminary pulse height distribution yields a mean value of ~11 ke. Since the calibration of the ROC has not been completed the exact value has yet to be determined.

2.3. FE-I4b read-out

The second prototype was connected to the FE-I4b ROC [15] with a 5 × 1 cell ganging due to its pitch of

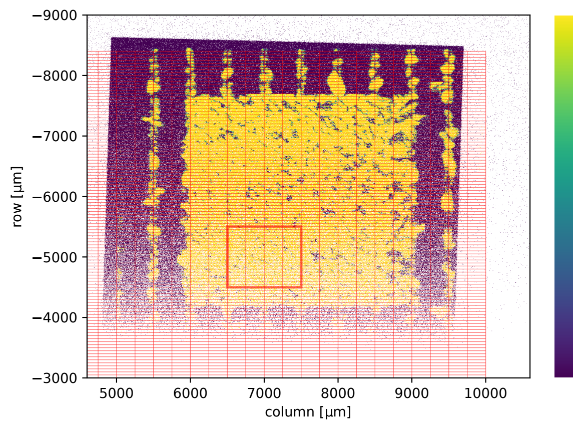

Figure 3: 5 × 1 efficiency

250 µm × 50 µm. The bump bonding was performed at IFAE-CNM in Barcelona by an adapted process with tin-silver bumps. Using a high resolution beam telescope with a spatial resolution of 3 µm at the device under test the efficiency could be mapped to the spatial coordinates. The results yield an efficiency of 97.8 % over the contiguous area in the red box (Figure 3). The missing efficiency is most likely due to issues with the bump bonding or the metallisation. Nevertheless the preliminary pulse height in the fiducial region already amounts to ~15 ke which is

consistent with the result of the first prototype considering the different momenta of the incident particles. A precise calibration for this ROC is also under way.

3. High Rate Studies

The HL-LHC will reach particle fluxes of $O\left(\mathrm{GHz/cm^2}\right)$ hence it is very important to understand the effect of the incident particle flux on the signal of pCVD diamonds. In order to conduct such a study it is essential to be able to vary the particle flux over a large range. The πM1 beam line at the High Intensity Proton Accelerator (HIPA) at PSI [16] can provide beams with continuously tunable fluxes from the order of 1 kHz/cm^2 up to 20 MHz/cm^2. The πM1 beam is a bunched beam with a spacing of 19.7 ns. For these studies a π^+ beam with with a momentum of 260 MeV/c was chosen in order to reach the highest possible flux [17].

3.1. Setup

The diamond sensors were connected in a pad geometry and prepared as described in [18]. In order to resolve single waveforms at high particle rates the sensors were connected to a fast, low-noise amplifier with a rise time of approximately 5 ns. The resulting waveforms were digitised and recorded in a beam telescope setup which provides spatial information of the hits in the diamond detector.

3.2. Results

pCVD diamond has a interior crystal structure where the single grains have slightly different properties. Therefore the size of the measured signal in pCVD depends also on the spatial position as can be seen in Figure 4. However this behaviour is constant and does not depend on time or rate.

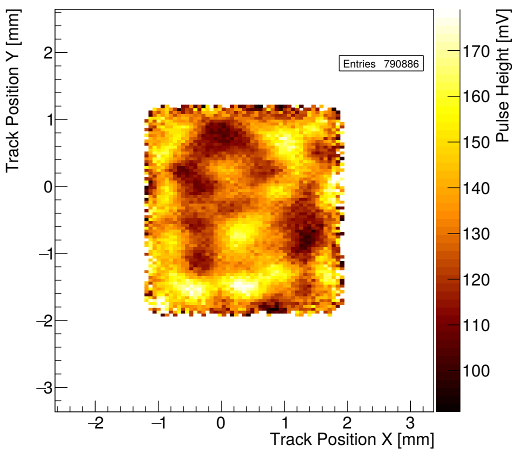

Figure 4: Signal map of a pCVD detector.

As an important factor also the beam induced current is studied depending on the particle rate. In 80 % of the measured diamonds the current is proportional to the flux and the leakage current (no beam) is of the O(1 nA). Some bad diamonds show shifting base lines or even erratic currents [19]. These are not shown in this article.

In order to measure the signal behaviour as a function of incident particle flux and irradiation, several rate scans with both polarities of the bias voltage were performed. Figure 5 shows the final results for a pCVD diamond with various fluences. The sensors were irradiated at the irradi-

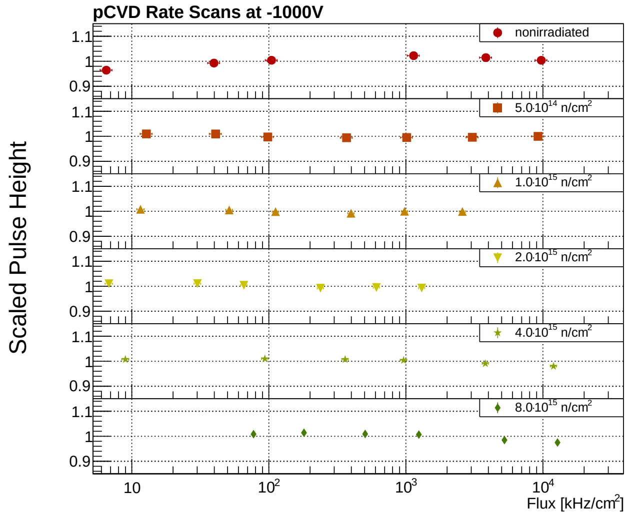

Figure 5: Pulse height versus incident particle flux for a pCVD diamond for various fluences at −1000 V.

ation facilities at the JSI TRIGA reactor in Ljubljana with fast reactor neutrons up to $8 \cdot 10^{15}$ n/cm^2 [20]. The mean of the single scans is scaled to 1. The pulse height is flat with the flux deviating less than 2 % from the mean up to a flux of 20 MHz/cm^2. We also observed a single diamond with a large rate dependence losing 90 % of the signal at highest rate. After the surface was processed with cleaning and Reactive Ion Etching (RIE), the device was reprocessed. A new measurement showed a deviation of less than 2 %. This leads us to the conclusion that this rate effect is due to surface issues and is possible to repair.

4. Conclusion

There is progress in the development of radiation tolerant particle detectors based on pCVD diamonds. The working principle of 3D pixel detectors was proven down to cell sizes of 50 µm × 50 µm and column diameters of 2.6 µm. The largest device has a number of 4000 cells. Already the first prototypes of small cell 3D detectors read out more charge than any planar pCVD diamond detector. The efficiency of the column drilling process is now above 99 %. The measured relative hit efficiency of the 3D pixel detectors reaches 99.3 % compared to a silicon device.

In extensive studies it was found that irradiated pCVD diamond detectors work reliably and show no signal dependence to the O(2 %) up to an incident particle flux of 20 MHz/cm^2. This was shown for an irradiation up to a fluence of $8 \cdot 10^{15}\,\mathrm{n/cm^2}$. The beam induced current of a pCVD diamond is proportional to the flux and the leakage current is of the $\mathcal{O}(1\,\mathrm{nA})$. A small fraction of the diamonds shows a large rate dependence which is most likely to surface issues and is possible to correct.

Acknowledgements

We want to thank the laser drilling team in Oxford around Patrick Salter for providing us with these great 3D detectors. Furthermore we want to thank Bert Harrop in Princeton and the team at IFAE for the great efforts in bump bonding our devices. Finally I also want to thank the rest of my collaboration for the advise and good cooperation.

References

[1] G. Apollinari, I. Béjar Alonso, O. Brüning, M. Lamont, L. Rossi, High-Luminosity Large Hadron Collider (HL-LHC): Preliminary Design Report, CERN Yellow Reports: Monographs, CERN, Geneva, 2015.
URL https://cds.cern.ch/record/2116337

[2] G. Auzinger, Upgrade of the CMS Tracker for the High Luminosity LHC, Tech. Rep. CMS-CR-2016-268, CERN, Geneva (Oct 2016).
URL https://cds.cern.ch/record/2227193

[3] H. Kagan, W. Trischuk, Development of Diamond Tracking Detectors for High Luminosity Experiments at the LHC, HL-LHC and Beyond, Tech. Rep. CERN-LHCC-2018-015. LHCC-SR-005, CERN, Geneva (May 2018).
URL https://cds.cern.ch/record/2320382

[4] W. de Boer, J. Bol, A. Furgeri, S. Müller, C. Sander, E. Berdermann, M. Pomorski, M. Huhtinen, Radiation hardness of diamond and silicon sensors compared, physica status solidi (a) 204 (9) (2007) 3004–3010. doi:10.1002/pssa.200776327.
URL http://dx.doi.org/10.1002/pssa.200776327

[5] H. Pernegger, V. Eremin, H. Frais-Kölbl, E. Griesmayer, H. Kagan, S. Roe, S. Schnetzer, R. Stone, W. Trischuk, D. Twitchen, P. Weilhammer, A. Whitehead, Charge-carrier properties in synthetic single-crystal diamond measured with the transient-current technique, J. Appl. Phys. 97 (7) (2005) 73704–1–9.
URL https://cds.cern.ch/record/909063

[6] S. Zhao, Characterization of the electrical properties of polycrystalline diamond films, Ph.D. thesis, The Ohio State University (1994).
URL http://wwwlib.umi.com/dissertations/fullcit?p9421043

[7] A. J. Edwards, B. Brau, M. Bruinsma, P. Burchat, H. Kagan, R. Kass, D. Kirkby, B. A. Petersen, M. Zoeller, Radiation monitoring with diamond sensors in babar, IEEE Transactions on Nuclear Science 51 (4) (2004) 1808–1811. doi:10.1109/TNS.2004.832634.

[8] R. Eusebi, R. Wallny, R. Tesarek, P. Dong, A. Sfyrla, W. Trischuk, C. Schrupp, A diamond-based beam condition monitor for the cdf experiment, 2006, pp. 709 – 712. doi:10.1109/NSSMIC.2006.355953.

[9] D. Schaefer, The ATLAS Diamond Beam Monitor: luminosity Detector on the LHC, Tech. Rep. ATL-INDET-PROC-2015-009, CERN, Geneva (Jul 2015).
URL https://cds.cern.ch/record/2034225

[10] S. Parker, C. Kenney, J. Segal, 3D - A proposed new architecture for solid-state radiation detectors, Nuclear Instruments and Methods in Physics Research Section A: Accelerators, Spectrometers, Detectors and Associated Equipment 395 (3) (1997) 328 – 343, proceedings of the Third International Workshop on Semiconductor Pixel Detectors for Particles and X-rays. doi:https://doi.org/10.1016/S0168-9002(97)00694-3.
URL http://www.sciencedirect.com/science/article/pii/S0168900297006943

[11] F. Bachmair, L. Bäni, P. Bergonzo, B. Caylar, G. Forcolin, I. Haughton, D. Hits, H. Kagan, R. Kass, L. Li, A. Oh, S. Phan, M. Pomorski, D. Smith, V. Tyzhnevyi, R. Wallny, D. Whitehead, A 3D diamond detector for particle tracking, Nuclear Instruments and Methods in Physics Research Section A: Accelerators, Spectrometers, Detectors and Associated Equipment 786 (2015) 97 – 104. doi:https://doi.org/10.1016/j.nima.2015.03.033.
URL http://www.sciencedirect.com/science/article/pii/S0168900215003496

[12] T. Kononenko, M. Komlenok, V. Pashinin, S. Pimenov, V. Konov, M. Neff, V. Romano, W. Lüthy, Femtosecond laser microstructuring in the bulk of diamond, Diamond and Related Materials 18 (2) (2009) 196 – 199, nDNC 2008 Proceedings of the International Conference on New Diamond and Nano Carbons 2008. doi:https://doi.org/10.1016/j.diamond.2008.07.014.
URL http://www.sciencedirect.com/science/article/pii/S0925963508003981

[13] B. Sun, P. S. Salter, M. J. Booth, High conductivity micro-wires in diamond following arbitrary paths, Applied Physics Letters 105 (23) (2014) 231105. arXiv:https://doi.org/10.1063/1.4902998, doi:10.1063/1.4902998.
URL https://doi.org/10.1063/1.4902998

[14] A. Kornmayer, T. Müller, U. Husemann, Studies on the response behaviour of pixel detector prototypes at high collision rates for the CMS experiment, presented 04 Dec 2015 (Nov 2015).
URL https://cds.cern.ch/record/2264667

[15] M. Garcia-Sciveres, D. Arutinov, M. Barbero, R. Beccherle, S. Dube, D. Elledge, J. Fleury, D. Fougeron, F. Gensolen, D. Gnani, V. Gromov, T. Hemperek, M. Karagounis, R. Kluit, A. Kruth, A. Mekkaoui, M. Menouni, J. Schipper, The FE-I4 Pixel Readout Integrated Circuit, Tech. Rep. ATL-UPGRADE-PROC-2010-001, CERN, Geneva (Jan 2010).
URL https://cds.cern.ch/record/1231359

[16] High Intesity Proton Accelerator at PSI, https://www.psi.ch/rf/hipa (2017).

[17] Pion and electron fluxes in piM1, http://aea.web.psi.ch/beam2lines/pim1c.html (2015).

[18] R. Wallny, et al., Beam test results of the dependence of signal size on incident particle flux in diamond pixel and pad detectors, JINST 10 (07) (2015) C07009.
URL https://cds.cern.ch/record/2159123

[19] M. Mikuz, V. Cindro, I. Dolenc, H. Kagan, G. Kramberger, H. Frais-Kolbl, A. Gorisek, E. Griesmayer, B. Macek, I. Mandic, M. Niegl, H. Pernegger, D. Smith, D. Tardif, W. Trischuk, P. Weilhammer, M. Zavrtanik, The atlas beam conditions monitor, Vol. 3, 2008, pp. 1914 – 1917. doi:10.1109/NSSMIC.2007.4436530.

[20] L. Snoj, G. Žerovnik, A. Trkov, Computational analysis of irradiation facilities at the jsi triga reactor, Applied Radiation and Isotopes 70 (3) (2012) 483 – 488. doi:https://doi.org/10.1016/j.apradiso.2011.11.042.
URL http://www.sciencedirect.com/science/article/pii/S0969804311005963